ASSESSING UNCERTAINTIES OF USING DAILY DATA OUTPUTS FROM REGIONAL NUMERICAL CLIMATE MODELS AS INPUTS INTO CROP SIMULATION MODELS

Guillermo A. Baigorria[1*], James W. Jones[1], D.W. Shin[2],
Ashok Mishra[3], and James J. O'Brien[2]

ABSTRACT

Regional numerical climate models may be able to produce climate forecasts that would provide useful predictions of crop yields several months in advance. In this study, we linked outputs from the Florida State University/Center for Ocean-Atmospheric Prediction Studies (FSU/COAPS) regional spectral model to a dynamic crop model (CERES-Maize) for evaluating uncertainties in yield prediction for three sites in the southeastern USA. Daily incoming solar radiation, maximum and minimum temperatures, and rainfall output data were obtained from an 18-year period of retrospective forecasts (hindcasts) that contained 20 realizations created by using two different convective schemes in the FSU/COAPS model. These raw hindcasts were bias-corrected by using cumulative probability functions from the historical daily weather record. The raw and bias-corrected hindcasts for each realization were compared to observed data at each selected site. Several combinations of the four meteorological variables from raw and bias-corrected hindcasts, as well as the climatological monthly values, were used as input in the crop model. Uncertainties related to all these combinations were analyzed. Mean, standard deviation and root mean squared error of rainfall for each ensemble member over the 18-year period were improved for bias-corrected daily data. Dry-spell length and frequency were also improved. The total squared error using the bias-corrected data mostly decreased for the other three meteorological variables in comparison to the raw hindcasts. Large variability in simulated yields among ensemble members was detected, mainly due to variability in timing of dry-spells during the cropping seasons.

Key words: Bias correction, crop models, downscaling, regional circulation models, yield forecast

INTRODUCTION

The Florida State University, Center for Ocean-Atmospheric Prediction Studies (FSU/COAPS) regional spectral model (Cocke and LaRow, 2000; Shin et al., 2006) coupled with the National Center for Atmospheric Research (NCAR) Community Land Model version 2 (CLM2; Bonan et al., 2002) may be useful for generating climate forecasts for Alabama, Florida, and Georgia. This coupled model improves the horizontal resolution of the seasonal surface climate outputs from ~200 km for the global model to ~20 km. (Shin et al., 2005, 2006). Two previously validated convective schemes were also included in the model in order to improve the simulation of the seasonal rainfall in the region (Shin et al., 2003): 1) the simplified Arakawa-

[1] Agricultural & Biological Engineering Department, U. of Florida., Gainesville, FL 32611-0570.
* Corresponding author e-mail: gbaigorr@ifas.ufl.edu
[2] Center for Ocean-Atmospheric Prediction Studies, The Florida State U., Tallahassee, FL 32312.
[3] International Research Institute for Climate and Society, Columbia U., Palisades, NY 10964.

Shubert (SAS; Pan and Wu, 1994) scheme from the National Center for Environmental Prediction; and 2) the relaxed Arakawa-Shubert (RAS) scheme developed in the Naval Research Laboratory (Rosmond, 1992).

Availability of high resolution forecasts produced from numerical models may provide opportunities for decision makers. Among them, agricultural related stakeholders are highly affected by the interannual variability of climate. Some of the most important cropping decisions are made at the beginning of the season, usually based on historical records (Hansen, 2002; Jagtap et al., 2002). Decisions as what, how, and when to plant are decisions that can not be changed during the cropping season (Baigorria, 2005, 2006; Jones et al., 2000). Dynamic crop models have been used in the last decade as tools for supporting decision makers by evaluating possible scenarios of interannual climate variability (Hansen and Indeje, 2004) and climate change (Dubrovský, 2000). For these applications, the El Niño Southern Oscillation (ENSO) index has played an important role in many regions of the world (Phillips et al., 1998; Podesta et al., 2002; Romero et al., in press). However, periods when ENSO phenomena have predictable effects on seasonal climate do not always match important cropping seasons (Hansen et al., 1999); this is why ENSO does not always have a clear effect on crop yields, especially in the northern hemisphere (Baigorria et al., submitted). Regional numerical models nested within Global Circulation Models (GCMs) have potential for improving forecasts because they predict large-scale circulation patterns that may influence local meteorological variables relative to use of ENSO phase alone. In the southeastern United States (SE USA) there is a weak predictability associated with ENSO during the Boreal summer growing season (Giannini et al., 2001; Higgins et al., 1998; Leathers, et al., 1991; Saravanan and Chang, 2000; Sutton et al., 2000). Our hypothesis is that the use of seasonal climate forecasts from numerical climate models in the SE USA will produce more reliable predictions of crop yields when coupled with dynamic crop models. However, it is necessary to know the uncertainties related to (*i*) the spatial and temporal downscaling of the seasonal climate forecast, and (*ii*) the integration effect of the crop model with seasonal climate forecasts treated as daily weather sequences.

Due to imperfect model specification and spatial averaging within GCM grid cells (Carter et al., 1994; Mearns et al., 1995; Goddard et al., 2001), numerical climate models overestimate the number rainfall events and do simulate short dry-spells during the simulated cropping season (Shin et al., 2006). This characteristic leads to an under-prediction of water stress and over-prediction of yields thus reducing interannual variability of yields (Dubrovský, 2000). Ines and Hansen (2006) proposed a method to correct biases in rainfall events and amounts using cumulative distribution functions. A two-step method adjusts the cumulative distribution functions of hindcast daily rainfall events and amounts outputs. There were also biases in hindcast incoming solar radiation, and maximum and minimum temperatures from the FSU/COAPS model (Shin et al., 2006).

This research was conducted to help answer several questions related to linking daily hindcast data from a regional climate model to a crop model. First, how much uncertainty is produced by feeding crop models with daily FSU/COAPS hindcast data of incoming solar radiation, maximum and minimum temperatures and rainfall? Is it possible to increase skill of crop yield predictions by using bias-corrected outputs from the FSU/COAPS model during the main corn growing season in the SE USA? How much uncertainty in crop yield forecasts is associated with each hindcast variable? Can daily climate forecast outputs be used as seasonal daily weather sequence forecasts? Objectives of this study were: 1) to quantify the uncertainty caused by using raw and bias-corrected hindcasts in dynamic crop model; and 2) to quantify

improvements in skill of applying bias corrections to daily hindcasts of the four selected daily meteorological variables.

DATA AND METHODS

Study area

The study area consists of the states of Alabama, Florida and Georgia in the SE USA between 35°23' N, 88°59' W and 24°57' N, 79°26' W. This region has some of the warmest conditions in the United States. The annual rainfall ranges from 1100 to 1400 mm, with the highest annual precipitation occurring along the Gulf of Mexico coast and in south Florida (USFS, 2006). Rainfall occurs throughout the year caused by two different processes. During most of fall and winter months, rainfall occurs mainly by fronts coming from the northwestern USA. During this frontal rainy season, spatial correlations among rainfall are characterized by a widely spread pattern in a northeast-southwest direction, perpendicular to the usual weather front paths (Baigorria et al., in press). During most of spring and summer months, rainfall occurs mainly by convective processes and tropical storms. During this convective rainy season spatial correlations among rainfall are characterized by small concentric patterns in which correlations decrease rapidly over short distances from each weather station (Baigorria et al., in press).

For the entire area, three counties with available weather and soil data, and where corn has been consistently cultivated during the last 18 years were selected for the current study (Figure 1). The counties were Alachua, FL, De Kalb, AL, and Tift, GA.

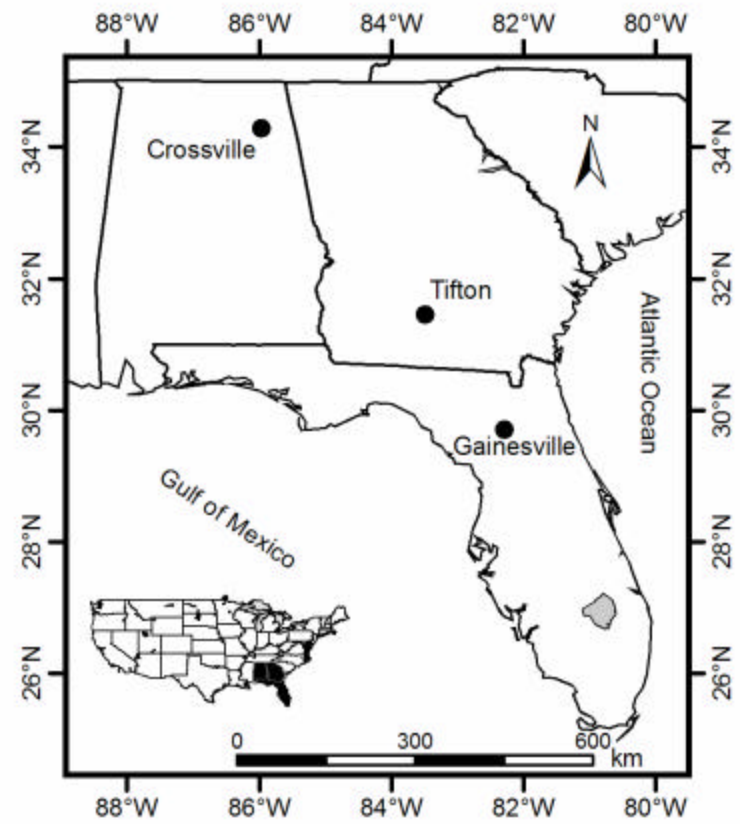

Figure 1. Locations of weather stations used in this research.

Data

Weather stations. One weather station located at each of the selected counties was used in this study: Gainesville in Alachua (29°42' N latitude, 82°17' W longitude, 38 m a.s.l.), Crossville in De Kalb (34°17' N latitude, 85°58' W longitude, 364 m a.s.l.), and Tifton in Tift (31°27' N latitude, 83°29' W longitude, 116 m a.s.l.). Daily data of maximum and minimum temperatures, and rainfall from these weather stations were obtained from the National Climate Data Center [http://nndc.noaa.gov/?home.shtml]. Incoming solar radiation was estimated using the technique of Richardson and Wright (1984). Monthly climatology values for these weather stations are shown in Table 1.

Table 1. Summary of climatic conditions observed at the three weather stations.

Month	Incoming solar radiation (MJ m^{-2} d^{-1})	Maximum temperature (°C)	Minimum temperature (°C)	Total rainfall (mm)	Number of rainy days
Gainesville, Alachua, Florida					
Mar	17.2	23.9	10.1	97.0	8.0
Apr	21.4	27.1	12.9	56.0	5.3
May	22.4	30.6	17.0	68.9	6.9
Jun	20.9	32.0	19.6	175.9	14.4
Jul	20.4	32.5	21.9	178.2	16.7
Aug	18.9	32.2	21.8	186.9	16.8
Sep	16.7	30.5	20.6	144.4	12.0
Crossville, De Kalb, Alabama					
Mar	14.5	17.1	4.2	200.9	14.7
Apr	18.5	21.8	8.8	159.1	12.5
May	21.6	25.7	13.4	149.1	13.0
Jun	22.7	29.2	17.4	140.0	12.4
Jul	22.3	30.9	19.2	144.3	13.2
Aug	20.4	30.8	18.5	116.2	11.9
Sep	16.9	27.8	15.3	156.1	11.2
Tifton, Tift, Georgia					
Mar	16.2	21.0	8.3	130.0	9.1
Apr	19.3	24.9	11.9	76.3	6.7
May	20.7	29.0	16.7	84.6	7.5
Jun	21.0	31.7	20.3	113.0	10.1
Jul	22.0	32.8	21.8	139.9	12.9
Aug	19.4	32.3	21.4	119.7	11.1
Sep	17.1	30.1	19.0	93.9	8.5

Retrospective forecast data (hindcasts). Daily output hindcasts of incoming solar radiation, maximum and minimum temperatures, and rainfall were taken from the realizations of the FSU/COAPS regional spectral model. Hindcast outputs corresponded to the 18-year period from 1987 to 2004, from April to September each year. A set of 20 realizations (ensembles members)

was generated by the FSU/COAPS model, and each ensemble was used in the analyses. These data were used to create the data files in the format used by the CERES-Maize corn model (Jones et al., 2003).

Soil data. Soil profile characteristics needed for crop simulations were obtained from the Natural Resources Conservation Service [www.nrcs.usda.gov]. Complete descriptions of chemical and physical properties from each soil profile by soil horizon used in this study are shown in Table 2.

Bias Correction

To correct daily rainfall amount and frequency, we used the bias-correction method based on the *gamma* cumulative probability function described by Ines and Hansen (2006). We extended this method to correct incoming solar radiation using the *beta* cumulative probability distribution and to correct minimum and maximum temperatures using the Gaussian cumulative probability distribution. Mathematical formulations used to bias-correct each meteorological variable are given below. The bias-correction method was applied to each ensemble member and for each month from March to September across the 18-year period. Table 3 describes variables used in this section.

Incoming solar radiation. The probability density function for the *beta* distribution can be written (Wilks, 2006):

$$f(x;p,q)=\left[\frac{\Gamma(p+q)}{\Gamma(p)\Gamma(q)}\right]x^{p-1}(1-x)^{q-1};\qquad 0\le x\le 1,\ p,q>0 \qquad [1]$$

$$\hat{p}=\frac{\bar{x}^2(1-\bar{x})}{s^2}-\bar{x};\quad \hat{q}=\frac{\hat{p}(1-\bar{x})}{\bar{x}} \qquad [2]$$

Because values of incoming solar radiation ranged from 0 to 33 MJ m^2 d^{-1} and the *beta* distribution is limited to the interval [0,1], a transformation is needed before its application by using:

$$\bar{x}'=\frac{\bar{x}-a}{b-a};\quad s_{x'}^2=\frac{s_x^2}{(b-a)^2} \qquad [3]$$

$\Gamma(l)$ is defined as the incomplete *gamma* function, and is estimated by:

$$\Gamma(l)=\int_0^\infty z^{l-1}e^{-z}dz \qquad [4]$$

The cumulative probability that a random variable x will be no larger than a specific incoming solar radiation value H is given by:

$$P(x\le H)=\int_0^H f(x;p,q)dx \qquad [5]$$

Table 2. Soil profile description in the simulated counties

Base layer depth (m)	Master Horizon	Wilting point ($cm^3\ cm^{-3}$)	Field capacity ($cm^3\ cm^{-3}$)	Max. water holding capacity ($cm^3\ cm^{-3}$)	Root growth factor	Saturated hydraulic cond. ($cm\ h^{-1}$)	Bulk density ($g\ cm^{-3}$)	Organic C ($g\ kg^{-1}$)	Clay ($g\ kg^{-1}$)	Silt ($g\ kg^{-1}$)	pH (water)	CEC ($cmol\ kg^{-1}$)
Alachua, Florida: Sand												
0.25	Ap	0.054	0.103	0.422	1.000	21.00	1.46	5.7	24	13	5.6	3.1
1.12	B1	0.044	0.085	0.404	0.100	21.00	1.52	1.6	28	18	5.1	1.8
1.57	B2	0.043	0.082	0.400	0.010	21.00	1.53	1.2	28	15	5.0	2.0
2.08	B3	0.060	0.102	0.390	0.001	21.00	1.56	1.2	61	20	5.1	3.4
2.21	B4	0.041	0.084	0.401	0.001	21.00	1.53	1.1	24	37	5.0	2.1
2.54	Bt	0.084	0.130	0.285	0.001	6.11	1.85	1.3	109	23	4.7	5.8
De Kalb, Alabama: Silt Loam												
0.15	Ap	0.083	0.244	0.514	1.000	0.68	1.21	15.3	53	514	5.7	4.5
0.33	B21t	0.116	0.282	0.506	0.670	0.68	1.23	4.5	181	557	4.8	5.6
0.61	B22t	0.132	0.296	0.503	0.390	0.68	1.24	3.4	224	534	4.7	6.3
0.94	B23t	0.129	0.281	0.467	0.060	1.32	1.34	1.2	214	471	4.7	7.1
1.78	B24t	0.162	0.308	0.456	0.001	0.23	1.37	0.2	288	402	4.6	8.0
Tift, Georgia: Loamy Sand												
0.25	Apc	0.093	0.183	0.432	1.000	6.10	1.42	11.4	72	130	5.6	2.6
0.51	Btc1	0.119	0.182	0.330	0.550	2.59	1.72	3.4	167	67	5.3	3.7
0.74	Btc2	0.149	0.212	0.353	0.200	0.43	1.66	2.4	232	62	5.7	3.6
1.02	Btcv	0.138	0.209	0.325	0.001	0.43	1.74	1.3	217	115	5.6	3.6
1.27	Btv1	0.177	0.245	0.339	0.001	0.43	1.70	1.8	292	74	5.3	4.6
1.63	Btv2	0.194	0.261	0.345	0.001	0.43	1.68	2.5	322	50	5.0	4.0
2.03	C	0.144	0.196	0.272	0.001	0.43	1.89	0.7	232	24	4.9	2.4

Bulk density estimated according to Rawls and Brakensiek (1985). Lower limit and Upper limit drained estimated according to Saxton et al. (1986). Upper limit saturated estimated according to Dalgliesh and Foale (1998) and Baumer and Rice (1988). CEC = cation exchange capacity.

Table 3. Variable descriptions.

Symbol	Definition	Units
x	Daily value	MJ m^2 d^{-1}, °C, or mm
$\overline{x}$	Mean	MJ m^2 d^{-1}, °C, or mm
n	Sample size	unitless
p, q	Parameters of the *beta* distribution	unitless
s	Standard deviation	
a, b	Minimum and maximum possible values of incoming solar radiation to truncate the *beta* distribution to the range [0,1]	MJ m^2 d^{-1}
x'	Transformed value	MJ m^2 d^{-1}
H	Incoming solar radiation	MJ m^2 d^{-1}
T	Temperature	°C
G	Incomplete *gamma* distribution	unitless
r	Rainfall	mm
a	Shape parameter of the *gamma* distribution	unitless
b	Scale parameter of the *gamma* distribution	unitless
X_i	Monthly hindcast value	MJ m^2 $month^{-1}$, °C, or mm $month^{-1}$
X_{obs}	Monthly observed value at weather station	mm $month^{-1}$
$\overline{X}_{obs}$	Monthly observed mean value at weather station	MJ m^2 $month^{-1}$, °C, or mm $month^{-1}$
$\overline{X}_{cli}$	Monthly observed climatological value	mm $month^{-1}$
$p(y_1,o_1)$	Join probability of hits	unitless
$p(y_2,o_2)$	Join probability of correct rejections	unitless
$p(o_i)$	Marginal distributions of the observations	unitless
$p(y_i)$	Marginal distributions of the forecasts	unitless
$F(x)$, $F_o(x)$	Cumulative probability of a hindcast (raw or corrected) and observed variable respectively	unitless

The inverse of the *beta* cumulative distribution was used to solve for specific x values by an iterative search technique. After bias correction, values of incoming solar radiation were checked to avoid values out of range. Values with less than 5% of the extraterrestrial radiation were replaced by this assumed minimum amount.

Maximum and minimum temperatures. The probability density function for the Gaussian distribution can be written (Wilks, 2006):

$$f(x;\overline{x},s) = \frac{1}{s\sqrt{2p}} e^{-\frac{(x-\overline{x})^2}{2s^2}}; \qquad -\infty \le x \le \infty \qquad [6]$$

To avoid minimum temperature values larger than maximum temperatures after applying the bias-correction, data from both variables were combined before fitting the Gaussian distribution. The cumulative probability that a random variable x will be no larger than a specific temperature value T is given by:

$$P(x \le T) = \int_0^T f(x)dx \qquad [7]$$

The inverse of the Gaussian cumulative distribution was used to solve for specific x values by an iterative search technique.

Rainfall frequency and amount. The correction of frequency of daily hindcast rainfall was performed by fitting a threshold value to truncate the cumulative distribution function of the raw daily hindcast rainfall. The threshold is calculated from the observed cumulative rainfall distribution function (Ines and Hansen, 2006).

The probability density function for the 2-parameter *gamma* distribution can be written as (Wilks, 2006):

$$f(x;a,b) = \frac{1}{b^a \Gamma(a)} x^{a-1} e^{-x/b}; \qquad x \ge \hat{x} \qquad [8]$$

Where a is the shape parameter and b is the scale parameter; both calculated based on the mean ($\bar{x}$) and variance (s^2) as:

$$a = \frac{\bar{x}^2}{s^2}; \quad b = \frac{s^2}{\bar{x}} \qquad [9]$$

The cumulative probability that a random variable x will be no larger than a specific rainfall value r is given by:

$$P(x \le r) = \int_0^r f(x;a,b)dx \qquad [10]$$

The inverse of the *gamma* cumulative distribution was used to solve for specific x values by an iterative search technique.

Measuring bias correction performance

Incoming solar radiation and temperatures. The total squared error (*TSE*) was used as accuracy measurement to compare cumulative probabilities of the raw and bias-corrected hindcast ($F[x]$) in relation to the observed cumulative probability ($F_o[x]$; Equation 11). To do so, we integrated the areas between the observed and hindcast curves across the range of cumulative probabilities and variable values.

$$TSE = \int_{-\infty}^{+\infty} \left[F(x) - F_o(x)\right]^2 dx \qquad [11]$$

Rainfall occurrence. To evaluate the performance of the bias-correction method on the daily rainfall occurrence in comparison with observed data, 2×2 contingence tables were used. Contingence tables were created for each ensemble member and for the entire season. Four possibilities were evaluated in the contingence tables: (*i*) hit – a rainfall event occurred and the hindcast was for a rainfall event; (*ii*) false alarms – a rainfall event was hindcast but did not occur; (*iii*) misses – a rainfall event occurred despite not being hindcast; and (*iv*) correct

rejections – no rainfall event occurred and the hindcast called for no rain. The Peirce Skill Score (*PSS*; Peirce, 1884) was used to summarize the square contingency tables. The *PSS* is interpreted as an improvement over a reference forecast, which in this case corresponds to the climatology. The *PSS* is calculated as:

$$PSS = \frac{p(y_1,o_1) + p(y_2,o_2) - p(y_1)p(o_1) - p(y_2)p(o_2)}{1 - p(o_1)p(o_1) - p(o_2)p(o_2)} \quad [12]$$

Perfect forecasts receive a score of one, random forecasts receive a score of zero and forecasts inferior to the random forecasts receive negative scores (Wilks, 2006).

Monthly rainfall amounts and number of rainy days. To evaluate the performance of the bias-correction method on total monthly rainfall and number of rainy days, mean and standard deviation across the 18-year hindcast period were calculated individually for each ensemble member. These statistics were calculated for both the raw and the bias-corrected hindcasts, and compared with data from the historical record. Root mean squared errors (RMSE) were calculated monthly for each ensemble member by using Equation 13.

$$RMSE_i = \sqrt{\frac{1}{n}\sum\left(X_i - \overline{X}_{obs}\right)^2} \quad [13]$$

A skill score (SS_{cli}; %) constructed using the mean squared error as the accuracy statistics was used. The SS_{cli} was computed using the climatological values as the reference forecast. In doing so, the SS_{cli} is the percentage improvement over climatology (Wilks, 2006). The range of SS_{cli} is from -100%, which indicates total lack of predictability in comparison with climatology, to 100%, which indicates maximum predictability relative to climatology.

$$SS_{cli} = 100 - \frac{\sum\left(X_i - \overline{X}_{obs}\right)^2}{\sum\left(X_{obs} - \overline{X}_{cli}\right)^2} \times 100 \quad [14]$$

Dry-spell length frequencies. Dry-spell length frequencies for the entire season were calculated for each ensemble member and compared graphically with observed and uncorrected data.

Linking crops and RNC models

Crop model. We selected the CERES-Maize model (Ritchie et al., 1998) because of the economical importance of corn in the region and because this crop is more sensitive to soil moisture deficit than other crops (Sadras and Calviño, 2001). Thus impacts of rainfall forecasts on crop yields can be evaluated relative to impacts of total rainfall amount and rainfall frequency.

The CERES-Maize model was used to simulate corn yield response under the different weather data sets. With the exception of planting date, crop management was set according to previous research in one of our study areas (Jones et al., 1986). The corn variety simulated was McCurdy 84AA, planted in a density of 7.2 plants m^{-2}. Planting date was the same every year, on 1 April in Crossville, AL and on 15 May in Gainesville, FL and Tifton, GA. Corn crops were simulated with no irrigation and with a total of 255 kg N ha^{-1} fertilizer split into 5 applications at 14-day intervals.

Each crop simulation used a single weather input level, soil profile (Table 2) and management practices. We did not evaluate the representativeness of the scenarios or account for heterogeneity of soils or weather.

The six evaluated weather input levels were: (*i*) raw hindcasts of all variables; (*ii*) bias-corrected hindcast of incoming solar radiation and raw hindcast of the remaining variables; (*iii*) bias-corrected hindcast of maximum and minimum temperatures and raw hindcast of the remaining variables; (*iv*) bias-corrected hindcast of rainfall and raw hindcast of the remaining variables; (*v*) bias-corrected hindcast of rainfall and climate monthly average of the remaining variables; and (*vi*) bias-corrected hindcast of all variables.

Measuring yield prediction performance. After crop simulations for all realizations were performed, yearly simulated dry matter yields were evaluated to measure the uncertainty of using different weather scenarios. Pearson's correlation and RMSE were computed for simulations using each weather scenario in comparison to the simulated results using observed weather data. Variability in annual yields for each hindcast ensemble member was analyzed for each weather scenario.

Results for one location and year were selected to analyze the effects of daily rainfall amounts and events in the crop simulation. To perform this analysis, the water stress factor affecting growth was used as a variable from the daily crop simulation outputs. The water stress factor affecting growth is a unitless index that ranges from 0 (no stress) to 1 (maximum stress; Hoogenboom et al., 2003). Daily values of water stress were transformed to binary data by assigning 1 to all values greater than 0 and 0 to the remaining values. This was done to analyze the temporal relationship between dry-spell distributions and crop yields.

RESULTS AND DISCUSSION

Bias correction analysis

Incoming solar radiation and temperatures. Comparing *TSE* values obtained from raw and bias-corrected hindcasts, it is apparent that the bias-correction of incoming solar radiation and minimum temperature reduced values of *TSE* for the three weather stations. However, bias-correction of maximum temperatures reduced *TSE* values only in Crossville and Tifton. The same analyses performed at a monthly level (results not shown), showed that the bias-correction for both temperatures fails when it is applied in Gainesville.

Rainfall. The *PSS*s (Peirce, 1884) values shown in Table 4 summarize contingency tables created by comparing occurrence of observed with hindcast events. As expected, rainfall occurrences were poorly forecast. According to the values shown, predictions were of the same *PSS* rank as random forecasts. These results are not surprising because the RCM were created to generate season-climate forecast and they are not daily weather forecasters. However, in this research where we used bias-corrected daily RCM outputs in dynamic crop models, this fact will play an important role in the results.

Bias-correction decreased the number of events by applying a threshold to achieve the historical record distribution (Ines and Hansen, 2006). Adjustments to the cumulative probability distributions resulted in good performance relative to correctly producing rainfall amounts across the studied months and to the entire season in comparison to the historical record. Over all ensembles, monthly and seasonal rainfall amounts averaged for the 18-year period showed values similar to the climatology. Standard deviations from the historical record were, in most of the cases, lower than those calculated from each ensemble member for the 18-year period.

Similar means and higher standard deviations than the climatology were due to some years being adjusted better than others. RMSE among the ensemble members ranged from 10.6 to 17.0% in rainfall amount and from 7.4 to 13.3% in number of rainy days. In most of the cases, SS_{cli} showed negative values. Positive values were lower than 8% for the total rainfall amount, and lower than 5% for number of rainy days taking into account the three weather stations and the 20 ensembles. This means that the climatology performed better than the bias-corrected hindcast.

Length and frequency of the dry-spells were adjusted adequately for the three weather stations using the bias corrections. An example for Gainesville for two different ensemble members is shown in Figure 2. Similar results were obtained for all of the ensemble members and weather stations.

Table 4. Peirce Skill Score (*PSS*) from daily bias corrected rainfall for three weather stations.

Member	Gainesville	Crossville	Tifton
1	0.040	-0.002	0.011
2	0.012	0.019	-0.011
3	0.012	0.010	0.047
4	0.045	-0.016	-0.009
5	0.041	0.013	0.031
6	0.047	0.020	0.009
7	0.064	0.026	-0.002
8	0.082	-0.016	0.023
9	0.055	-0.010	0.028
10	0.025	-0.034	0.008
11	0.041	-0.028	0.009
12	0.033	0.034	0.015
13	0.082	-0.008	0.002
14	0.028	-0.042	0.010
15	0.038	0.015	-0.011
16	0.045	-0.010	-0.003
17	0.039	0.013	0.016
18	0.040	-0.044	-0.002
19	0.008	0.011	-0.002
20	0.018	-0.027	-0.024

Linking FSU/COAPS and CERES-Maize models

Figure 4 shows the comparison maize yields using the raw hindcasts of all variables (a) versus the bias-corrected hindcasts of all variables (f), as well as the effects individual bias-corrected variables (b to e). The lowest RMSE value was found when rainfall was bias-corrected in combination with raw hindcasts of incoming solar radiation and maximum and minimum temperatures (Figure 3d). When these three raw hindcast variables were replaced by the climatological values as originally performed by Ines and Hansen (2006), RMSE values increased and the Pearson's correlations decreased (Figure 3e).

Bias-correcting maximum and minimum temperatures increased simulated corn yields compared with the raw hindcast of all variables (Figure 3c and 3a respectively); RMSE increased and Pearson's correlations decreased. As shown in Figure 4, the FSU/COAPS regional spectral model overestimated temperatures. Bias-correcting maximum and minimum temperatures decreased these values, decreasing the simulated evapotranspiration rates. This correction diminished length of dry-spells, thereby reducing the water deficit and increasing simulated yields.

Bias-correction of incoming solar radiation also increased RMSE and decreased Pearson's correlations compared to the raw hindcast of all variables (Figure 3b and 3a, respectively). Bias-correcting incoming solar radiation slightly increased the range of variation among the ensemble members in comparison to the raw hindcast of all variables.

Comparisons of Pearson's correlation and RMSE values between simulated yields using raw and bias-corrected hindcasts of all variables are shown in Table 5 for the 20 ensemble members and their average. Predictability among the ensemble members varied considerably. In Gainesville, a maximum of 33% of the interannual variability was explained by ensemble member 15 from the raw hindcasts of all variables. Predictability of ensemble member 15 decreased to 18% after the application of bias-correction to all variables. However,

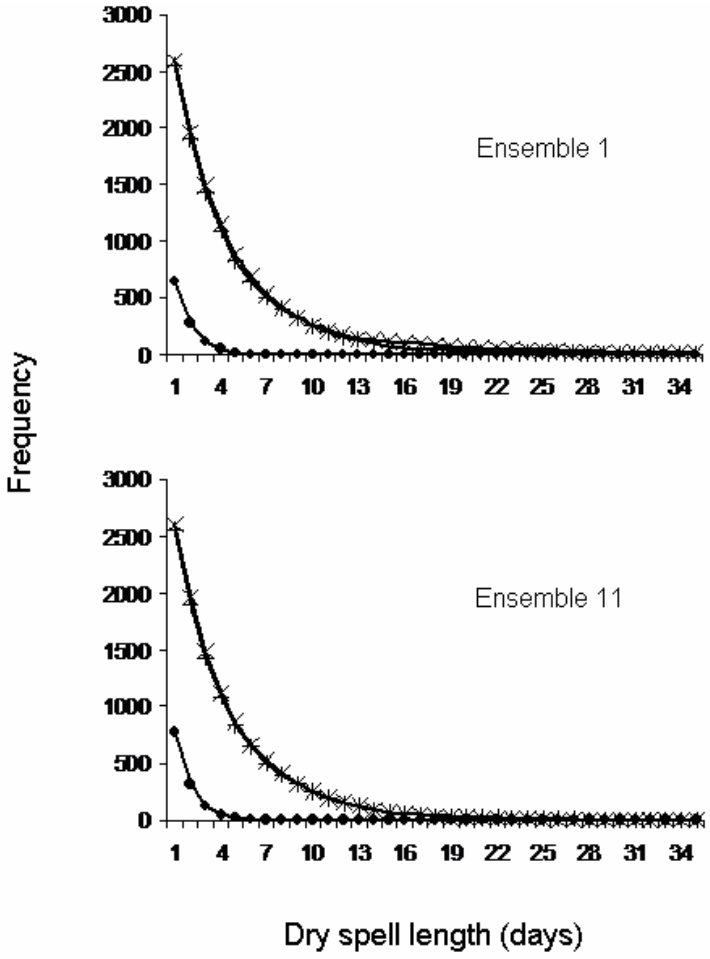

Figure 2. Dry-spell length frequencies comparison among observed (+), raw hindcast (•), and bias corrected (X) rainfall data.

ensemble member 16 performed the best among the ensemble members predicting 32% of the interannual variability after the application of bias-correction of all variables. In Crossville, a maximum of 24% of the interannual variability was explained by ensemble member 15 from the raw hindcast of all variables. After bias-correcting all variables, ensemble member 16 explained 16% of the interannual variability. In most of the cases, Pearson's correlation decreased and RMSE increased across the ensemble members when all variables were bias-corrected. RMSE values ranged from 51 to 74% among ensembles members for raw hindcasts and from 56 to 80% for bias-corrected hindcasts. In Tifton, Pearson's correlation increased and RMSE decreased after bias-correction of all variables. A maximum of 31% the interannual variability was explained by ensemble member 12 using raw data compared with a maximum 46% using bias-corrected data.

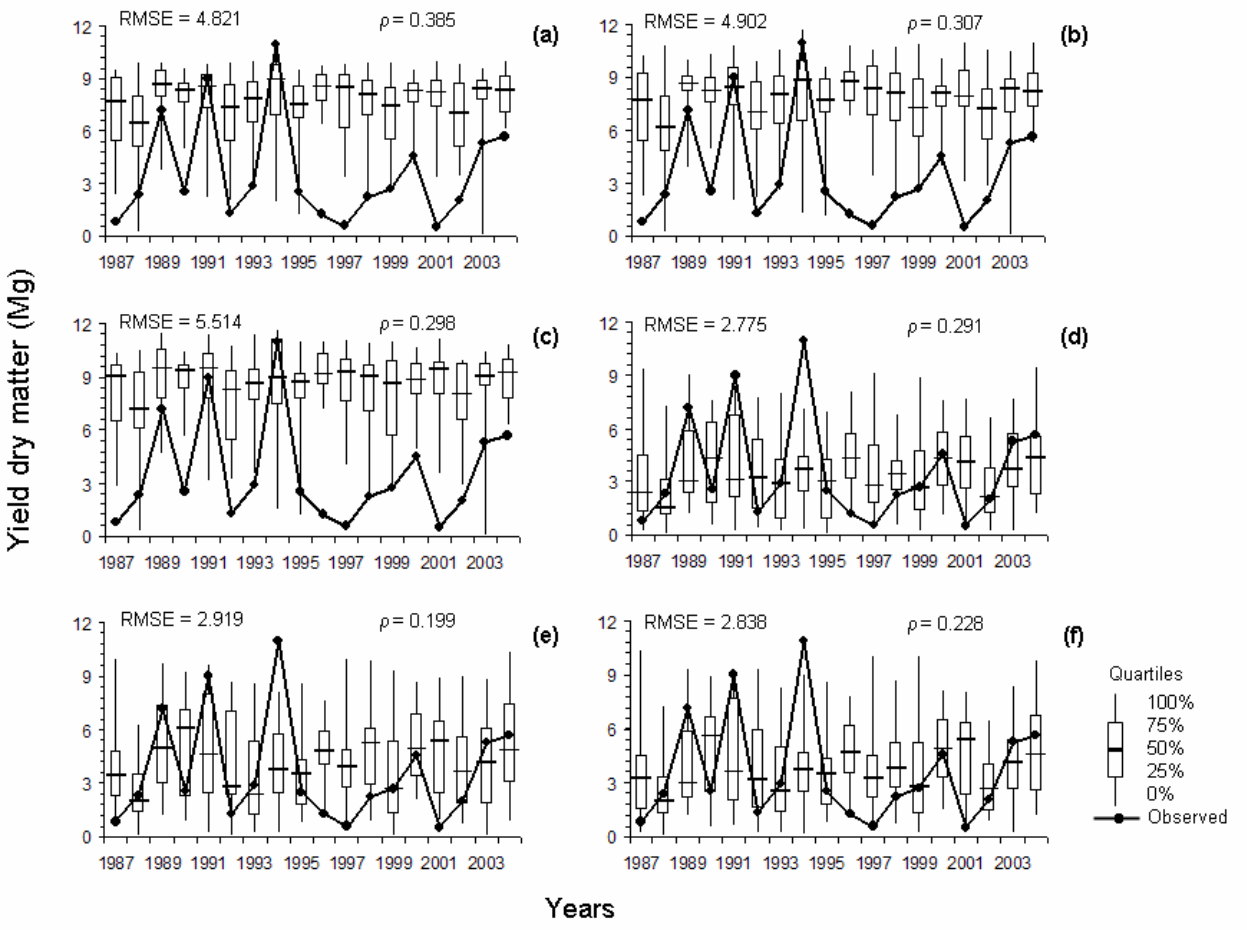

Figure 3. Comparison of the crop simulation scenarios between simulated corn yield dry matter using observed weather in Tifton (•) and ensemble members' quartiles of: a) raw hindcast of all variables; b) bias-corrected hindcast of incoming solar radiation and raw hindcast of the remaining variables; c) bias-corrected hindcast of maximum and minimum temperatures, and raw hindcast of the remaining variables; d) bias-corrected hindcast of rainfall and raw hindcast of the remaining variables; e) bias-corrected hindcast of rainfall and climate monthly average of the remaining variables; and f) bias-corrected hindcast of all variables.

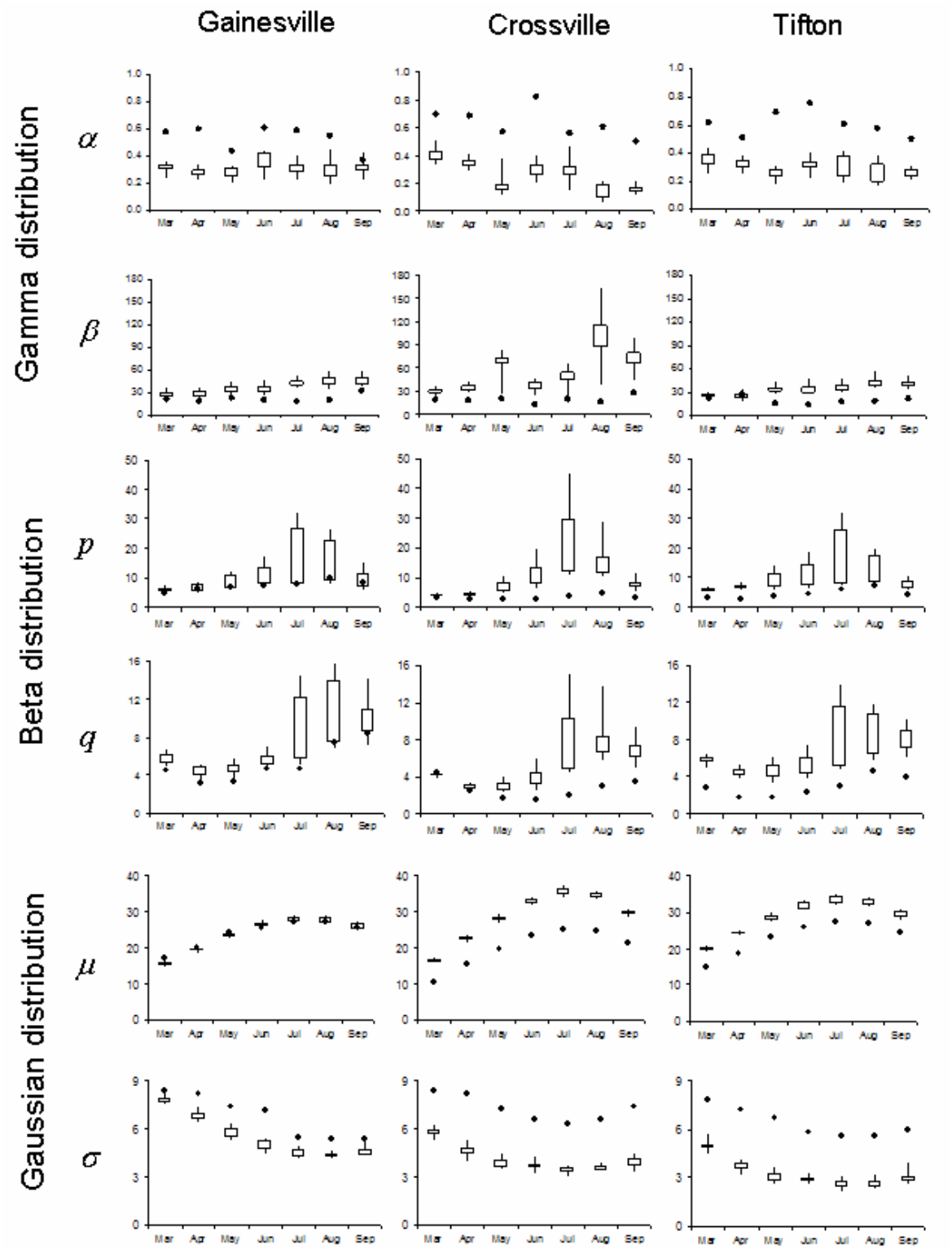

Figure 4. Monthly variability of the parameters of the *gamma* (rainfall), *beta* (incoming solar radiation), and Gaussian (maximum and minimum temperatures combined) distributions fitting the daily data at weather station level (•) and the raw hindcast from the 20 ensemble members (0, 25, 75, and 100 percentile).

Table 5. Pearson's correlation (*?*) and root mean square error (RMSE) between simulated corn dry matter yields using observed weather and each bias-corrected hindcast of all variables ensemble members. Highest positive correlations are bold.

Ensemble member	Gainesville				Crossville				Tifton			
	Raw hindcast		Bias-corrected hindcast		Raw hindcast		Bias-corrected hindcast		Raw hindcast		Bias-corrected hindcast	
	?	RMSE	?	RMSE	?	RMSE	?	RMSE	?	RMSE	?	RMSE
1	-0.0148	3.543	0.1103	3.012	-0.1870	5.157	-0.2072	5.625	0.1729	5.289	-0.0236	3.827
2	0.1921	3.185	0.2652	3.154	0.1341	5.333	0.0462	5.520	0.4854	4.457	0.2127	3.497
3	0.0494	3.232	0.5466	2.628	-0.2691	5.054	-0.2598	5.651	-0.2836	5.255	-0.2318	4.392
4	0.0237	3.518	0.1270	4.028	-0.1731	5.576	-0.4669	6.010	-0.3862	5.477	-0.1162	3.900
5	0.1656	3.419	0.0783	3.341	0.0409	5.500	0.0047	6.208	-0.0688	5.055	-0.0768	4.128
6	-0.2282	3.738	-0.6093	4.092	-0.3578	5.763	-0.1555	5.833	-0.0486	5.175	-0.1036	3.694
7	-0.1171	3.472	-0.1667	3.884	0.0256	5.082	0.1780	5.447	-0.0456	4.986	0.0900	3.874
8	0.4392	3.086	0.3734	2.714	-0.0077	5.389	0.0906	5.313	-0.2245	5.676	-0.5512	4.500
9	0.0078	3.327	0.2140	3.227	0.0847	5.764	0.1491	5.208	0.1473	5.239	0.1108	3.589
10	-0.1801	4.003	-0.0200	3.224	-0.2460	5.847	-0.3480	5.323	0.0465	5.505	-0.0506	3.673
11	0.3086	3.536	0.1936	2.876	-0.0029	4.821	0.0189	5.409	0.4552	4.821	0.2827	3.030
12	0.1261	3.794	-0.0684	3.772	-0.0631	5.197	-0.0598	5.561	**0.5528**	4.489	**0.6784**	2.158
13	0.3719	3.396	0.5168	2.749	0.1728	4.579	0.1408	4.799	0.3409	5.321	0.5102	2.619
14	-0.0725	3.782	-0.3061	3.718	-0.3123	5.746	-0.3971	5.913	0.0249	5.495	0.2328	3.137
15	**0.5754**	2.929	0.4254	2.583	**0.4896**	3.828	0.3598	4.375	0.4662	4.712	0.2804	3.462
16	0.5437	3.451	**0.5610**	2.196	0.3349	4.689	**0.4036**	4.882	0.0785	5.283	-0.2443	4.403
17	-0.0723	3.529	0.0689	3.023	-0.0391	4.882	-0.1625	5.510	0.1471	5.161	0.2191	3.228
18	0.0533	3.674	-0.0026	3.418	-0.1971	5.215	-0.1059	5.415	-0.0293	5.356	0.0558	3.658
19	0.1582	3.792	-0.0333	3.111	0.4551	4.303	0.3740	4.147	0.0941	5.788	-0.3798	4.572
20	0.0096	3.946	-0.3411	4.023	-0.2129	5.636	-0.0944	5.195	0.3718	4.985	0.5165	2.601
$\overline{X}$	0.2823	3.281	0.3206	2.550	-0.0184	4.697	-0.0649	4.538	0.3853	4.821	0.2275	2.838

$\overline{X}$ = average dry matter from the 20 ensemble members.

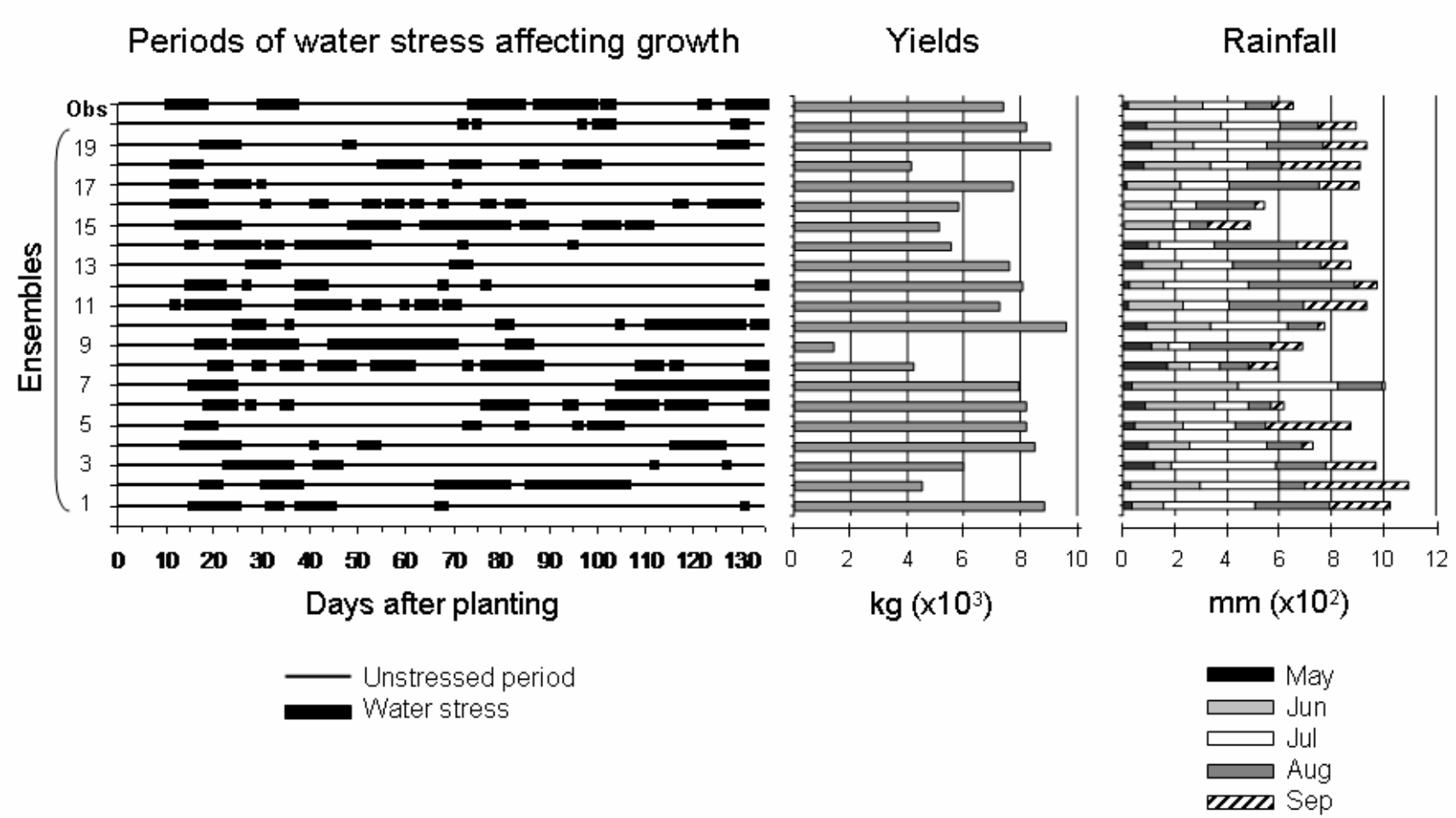

Figure 5. Case study comparing observed and hindcast ensemble members of simulated periods under water stress affecting growth and it relationship to dry matter yields and total monthly rainfall. Gainesville 1990.

Yields simulated by dynamic crop models were highly sensible to dry-spell sequences during the cropping season. Dubrovský et al. (2000) reported that increasing persistence of wet or dry day occurrence resulted in an increasing probability of drought, which was accompanied by decreased mean and increased variance of grain yields. According to our results, in addition to increasing persistence of wet or dry day occurrence was important, timing of wet- or dry-spells within the cropping season was especially important. Figure 5 graphically compares the total and monthly amounts of rainfall during the cropping season versus yields and versus the stress factor affecting growth during the cropping season. As an example, ensemble member 2 received most rain, however, it showed one of the smallest simulated yields. This result was because a long dry-spell occurred just before and during tasseling, the most drought sensitive physiological stage for producing corn. The opposite occurred in ensemble member 6 where the total rainfall amount was in the below-normal tercile, but simulated yields were in the above-normal tercile. In this case, most of the water deficit occurred after the grain-filling phase when water did not play an important role in yield.

As explained above, there was no apparent physical explanation for the observation that some ensemble members performed better than others. Moreover, these good-performer members varied by location, so they could not be selected for an operational forecast.

Curiously, most outliers in simulated yields using observed data were produced during neutral years. Most of the simulated yields using observed data under the El Niño and the La Niña conditions were simulated within the variability of the ensemble members after bias-correcting the hindcasts to all the variables. This result indicates that the FSU/COAPS regional spectral model simulated climate better during El Niño and La Niña years than during neutral years when uncertainty increased.

CONCLUSIONS

Bias correction of climate models outputs based on cumulative distribution functions of historical data improved the quality of daily hindcast data provided by the FSU/COAPS regional spectral model. However, interannual variability was not adequately corrected and some years were adjusted better than others. Dry-spell length and frequency were also adequately corrected over the 18-year period of record by the method; however the dry-spell distribution within a growing season, as expected, was not well simulated.

There was a large variability among the ensemble member yield predictions. Some ensemble members were better than others at representing interannual variability of simulated yields using observed data; however there was no physical basis to select them as individual predictors. Differences in dry-spell distribution within the cropping season were the main source of uncertainty using the bias correction method in this study. As a consequence, daily seasonal climate forecasts from the FSU regional spectral model could not be taken as an all-season weather sequence forecasts to feed dynamic crop models from the DSSAT crop system modeling group.

ACKNOWLEDGEMENTS

The research was supported by the National Oceanic and Atmospheric Administration – Applied Research Center (NOAA-ARC) through the grant No. NA16GP1365 subcontract FSU/UF No. 02081352-1-1 and developed under the auspices of the Southeast Climate Consortium (SECC). The views expressed in this paper are those of the authors and do not necessarily reflect the views of NOAA or any of its sub-agencies.

REFERENCES

Baigorria GA. 2005. Weather and seasonal climate forecast to support agricultural decision-making at different spatial and temporal scales. In: Baigorria GA, Climate interpolation for land resource and land use studies in mountainous regions. PhD thesis dissertation. Wageningen University and Research Centre, Wageningen, the Netherlands. p. 71-96.

Baigorria GA. 2006. Assessing the use of seasonal-climate forecasts to support farmers in the Andean Highlands. In: Sivakumar MVK, Hansen JW (Eds). Climate prediction and agriculture: Advances and Challenges. WMO/START/IRI, Geneve, Switzerland.

Baigorria GA, Hansen JW, Ward N, Jones JW, O'Brien JJ. 2006. Regional atmospheric circulation and surface temperatures predicting cotton yields in the Southeastern USA. J. App. Meteorol. (Submitted)

Baigorria GA, Jones JW, O'Briend JJ. Understanding rainfall spatial variability in the Southeast USA at different timescales. Int J Climatol Doi: 10.1002/joc.1435. In press

Baumer OW, Rice JW. 1988. Methods to predict soil input data for DRAINMOD. Am Soc Agr Eng Paper 88-2564.

Bonan GB, Oleson KW, Vertenstein M, Levis S, Zeng X, Dai Y, Dickinson RE, Yang Z-L. 2002. The land surface climatology of the Community Land Model coupled to the NCAR Community Climate Model. J. Climate 25:3123-3149.

Carter TR, Parry ML, Harasawa H, Nishioka S. 1994. IPCC technical guidelines for assessing climate change impacts and adaptations. Special Report to Working Group II, Intergovernment Panel on Climate Change.

Cocke S, LaRow TE. 2000. Seasonal predictions using a regional spectral model embedded within a coupled ocean-atmosphere model. Mon. Weather. Rev. 128:689-708.

Dalgliesh NP, Foale MA. 1998. Soil Matters – monitoring soil water and nitrogen in dryland farming. CSIRO, Agricultural Production Systems Research Unit, Toowoomba, Queensland, Australia.

Dubrovský M, Zalud Z, Stastna M. 2000. Sensitivity of CERES-maize yields to statistical structure of daily weather series. Climate Change 46:447-472.

Giannini A, Chiang JCH, Cane MA, Kushnir Y, Seager R. 2001. The ENSO teleconnection to the Tropical Atlantic Ocean: Contributions of the remote and local SSTs to rainfall variability in the Tropical Americas. J. Climate 14:4530-4544.

Goddard L, Mason SJ, Zebiak SE, Ropelewski CF, Basher R, Cane MA. 2001. Current approaches to seasonal to interannual climate predictions. Int. J. Climatol. 21:1111-1152.

Hansen JW. 2002. Realizing the potential benefits of climate prediction to agriculture: issues, approaches, challenges. Agric. Sys. 74:309-330.

Hansen JW, Indeje M. 2004. Linking dynamic seasonal climate forecasts with crop simulation for maize yield prediction in semi-arid Kenya. Agric. Forest Meteorol. 125:143-157.

Hansen JW, Jones JW, Kiker CF, Hodges AW. 1999. El Niño-Southern Oscillation impacts on winter vegetable production in Florida. J. Climate 12:92-102.

Higgins RW, Mo KC, Yao Y. 1998. Interannual variability of the U.S. summer precipitation regime with emphasis on the Southwestern Monsoon. J. Climate 11:2582-2606.

Hoogenboom G, Jones JW, Porter CH, Wilkens PW, Boote KJ, Batchelor WD, Hunt LA, Tsuji GY (Eds.). 2003. Decision Support System for Agrotechnology Transfer Version 4.0. University of Hawaii, Honolulu, HI.

Ines AVM, Hansen JW. 2006. Bias correction of daily GCM rainfall for crop simulation studies. Agric. Forest Meteorol. 138:44-53.

Jagtap SS, Jones JW, Hildebrand P, Letson D, O'Brien JJ, Podestá G, Zierden D, Zazueta F. 2002. Responding to stakeholder's demands for climate information: from research to applications in Florida. Agric. Sys. 74:15-430.

Jones JW, Hansen JW, Royce FS, Messina CD. 2000. Potential benefits of climate forecasting to agriculture. Agr. Ecosyst. Environ. 82:169-184.

Jones JW, Hoogenboom G, Porter CH, Boote KJ, Batchelor WD, Hunt LA, Wilkens PW, Singh U, Gijsman AJ, Ritchie JT. 2003. The DSSAT cropping system model. Eur. J. Agron. 18:235-265.

Jones JW, Zur B, Bennett JM (1986) Interactive effects of water and nitrogen stresses on carbon and water vapor exchange of corn canopies. Agric Forest Meteorol 38:113-126

Leathers DJ, Yarnal B, Palecki MA. 1991. The Pacific/North American teleconnection pattern and United States Climate. Part I: Regional temperature and precipitation associations. J. Climate 4:517-528.

Mearns LO, Giorgi F, McDaniel L, Shields C. 1995. Analysis of daily variability of precipitation in a nested regional climate model: comparison with observations and doubled CO_2 results. Global Planet Change 10:55-78.

Pan HL, Wu WS. 1994. Implementing a mass flux convection parameterization scheme for the NMC Medium Range Forecast Model. 10th Conf. on Numerical Weather Prediction. Amer. Meteor. Soc. p 96-98.

Peirce CS. 1884. The numerical measure of the success of predictions. Science 4:453-454.

Phillips JG, Cane MA, Rosenzweig C. 1998. ENSO, seasonal rainfall patterns, and simulated maize yield variability in Zimbabwe. Agric For Meteor 90:39-50.

Podestá G, Letson D, Messina C, Royce F, Ferreyra RA, Jones JW, Hansen JW, Llovet I, Grondona M, O'Brien JJ. 2002. Use of ENSO-related climate information in agricultural decision making in Argentina: a pilot experience. Agric. Sys. 74:371-392.

Rawls WJ, Brakensiek DL. 1985. Prediction of soil water properties for hydrologic modeling. pp. 293-299 *In*: Jones EB, Ward TJ (Eds.), Proc. Symp. Watershed Management in the Eighties. Am. Soc. Civil Eng., New York, NY.

Richardson CW, Wright DA. 1984. WGEN: A model for generating daily weather variables. U.S. Department of Agriculture, Agricultural Research Service. Publication ARS-8.

Ritchie JT, Singh U, Godwin DC, Bowen WT. 1998. Cereal growth, development and yield. pp. 79-98. *In:* Tsuji GY, Hoogenboom G, Thornton PK (Eds). Understanding Options for Agricultural Production. Kluwer Academic Publishers, Dordrecht, the Netherlands.

Romero CC, Baigorria GA, Stroosnijder L. 2006. Changes of erosive rainfall for El Niño and La Niña years in the northern Andean Highlands of Peru. Climatic Change (In press)

Rosmond TE. 1992. The design and testing of the Navy Operational Global Atmospheric Prediction System. Weather Forecasting 7:262-272

Sadras VO, Calviño PA. 2001. Quantification of grain yield response to soil depth in soybean, maize, sunflower, and wheat. Agron. J. 93:577-583.

Saravanan R, Chang P. 2000. Interaction between Tropical Atlantic variability and El Niño-Southern Oscillation. J. Climate 13:2177-2194

Saxton KE, Rawls WJ, Romberger JS, Papendick RI. 1986. Estimating generalized soil-water characteristics from texture. Soil Sci. Soc. Am. J. 50:1031-1036

Shin DW, Below JG, LaRow TE, Cocke S, O'Brien JJ. 2006. The role of an advance land model in seasonal dynamical downscaling for crop model application. J. Appl. Meteorol. Climatol. 45:686-701

Shin DW, Cocke S, LaRow TE, O'Brien JJ. 2005. Seasonal surface air temperature and precipitation in the FSU Climate Model coupled to the CLM2. J Climate 18:3217-3228.

Shin DW, LaRow TW, Cocke S. 2003. Convective scheme and resolution impacts on seasonal precipitation forecasts. Geophys. Res. Lett. 30:2078

Sutton RT, Jewson P, Rowell DP. 2000. The elements of climate variability in the Tropical Atlantic Region. J. Climate 13:3261-3284.

Wilks DS (2006) Statistical methods in the atmospheric sciences. Internat. Geophys. Series (2nd Ed.) Elsevier Academic Press Publications, CA